

## Dynamic Recompartmentalization of Supported Lipid Bilayers Using Focused Femtosecond Laser Pulses

Andreia M. Smith,<sup>†,¶</sup> Thomas Huser,<sup>\*,§,¶</sup> and Atul N. Parikh<sup>\*,†,‡,¶</sup>

Applied Science, Biophysics, and Internal Medicine Graduate Programs, and NSF Center for Biophotonics, Science and Technology, University of California, Davis, California 95619

Received August 3, 2006; E-mail: trhuser@ucdavis.edu; anparikh@ucdavis.edu

Lateral dynamics of lipids and proteins at cellular surfaces have a far-reaching influence on many biological processes.<sup>1</sup> A growing body of evidence now suggests that these lipids and proteins display a broad variation in molecular diffusivities,<sup>2</sup> determined by membrane heterogeneities (e.g., proteins, multiprotein aggregates, and cytoskeleton-binding proteins) and membrane compartmentalization.<sup>1,3</sup> Moreover, these heterogeneities (and compartments) themselves rearrange, further complicating molecular mobilities within membranes.<sup>1–3</sup> How the presence, distributions, and dynamics of diffusional barriers influence Brownian motions of lipids and proteins, however, remains poorly understood. To systematically study these processes, model systems which exhibit dynamic membrane compartmentalization are highly desirable.

In a parallel line of research, ultrafast laser pulses (e.g., femtosecond) are proving to be valuable in inducing highly localized photomodifications in many soft materials including glasses, polymers, and cells.<sup>4</sup> In biomaterials, their applications include dissection of sub-cellular structures for nerve regeneration and targeted transfections via transient perforation of plasma membranes.<sup>5</sup> All of these applications depend on high peak intensities ( $> 10^{13}$  W/cm<sup>2</sup>) achieved within the focal volume under low-energy conditions, thus inducing multiphoton absorptions. This, in conjunction with cascade ionization, produces very high concentrations of free electrons, thus facilitating plasma-mediated molecular degradation within the diffraction limit.<sup>4</sup>

We used a tunable Ti:sapphire laser operating at 800 nm (350 fs pulse-width) and with a tunable repetition rate (56 MHz to 2.7 kHz). The laser output was coupled into an inverted optical microscope and focused into a diffraction-limited spot by a Nikon 100X/1.45 NA oil objective (see Supporting Information). A supported membrane composed of POPC (1-palmitoyl-2-oleoyl-*sn*-glycero-3-phosphocholine) doped with 1 mol % of Texas Red/DHPE (Texas Red 1,2-dihexadecanoyl-*sn*-glycero-3-phosphoethanolamine triethylammonium salt) on a coverglass was prepared following the vesicle spreading and rupture method (Supporting Information). The bilayer was maintained wet by sandwiching the sample with a DI water-filled hanging drop slide.

Initially, the fluorescence signal due to Texas Red is bright and spatially homogeneous (Figure 1a), confirming the formation of a fluid POPC bilayer. Exposure to the femtosecond pulses at the low repetition rate of 2.7 kHz at 3 nJ pulse energy for 100 ms produces a dark blurry spot ( $\sim 2$   $\mu$ m fwhm) in the fluorescent bilayer (Figure 1b). Within several seconds, this spot fades away and is replaced by a stable, 330 nm diameter, fluorescence-free void within the illumination field (Figure 1c). The initial darkened spot can be attributed to photobleaching induced by the two-photon excitation of the Texas Red/DHPE. Its subsequent recovery confirms sustained

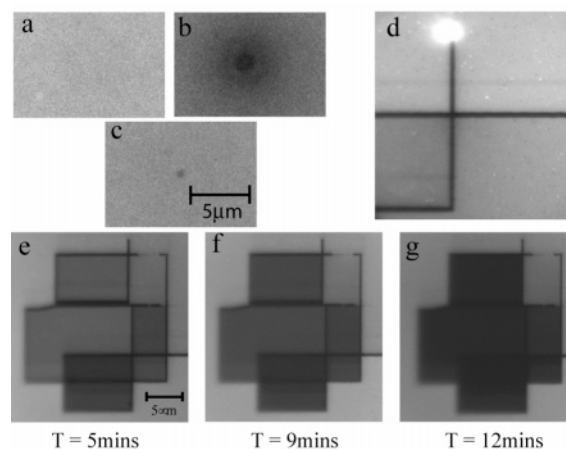


**Figure 1.** (a–c) Epifluorescence images of the optoporation process of a POPC bilayer (doped with 1 mol % of Texas Red/DHPE) supported on glass substrates. (d) Image of the laser illumination spot whose lateral translation produces a continuous trail of fluorescence-free voids. (e–g) Selected images of a time-lapse photobleaching sequence confirming the confinement of lipids.

fluidity of the residual bilayer after the laser exposure. The permanent fluorescence-free area is consistent with the formation of a physical void further confirmed by the adsorption of bovine serum albumin (BSA) (Supporting Information).

We observe that these localized voids only form when the laser pulse energies reside in a narrow range of 3–6 nJ under our focusing conditions. Below pulse energies of 3 nJ, the diffusive spot fully blends in with the fluorescent background within a few seconds, but no stable void is formed. In contrast, for pulse energies above 6 nJ, a large, non-uniform region devoid of fluorescence is observed, suggesting extensive collateral damage to the bilayer (Supporting Information). At these energies, little damage to the glass substrate occurs (Supporting Information). The bilayer optoporation under optimal conditions of 3–6 nJ is independent of the bilayer composition, fluidity, or fluorophore, further confirming the generality of the process.

The point barriers formed by the optoporation process can be extended to create arbitrary line (1D) patterns of diffusional barriers by simply translating the sample laterally under a continuous exposure to the laser beam (Figure 1d). We find that a local dwell time as low as 2.5 ms is sufficient to achieve a 1D perforation of our bilayers. In this manner, continuous line barriers over large sample areas can be easily fabricated in several seconds. An example is shown in Figure 1e–g, which shows time-lapse fluorescence images of a barrier pattern comprising “open” and “closed” boxes. Upon prolonged illumination by a Hg lamp, closed boxes become dark, whereas the open box remains fluorescent, indicating that the barrier pattern confines the lipids within the

<sup>†</sup> Department of Applied Science.

<sup>‡</sup> Biophysics Graduate Group.

<sup>§</sup> Department of Internal Medicine.

<sup>¶</sup> NSF Center for Biophotonics Science and Technology.

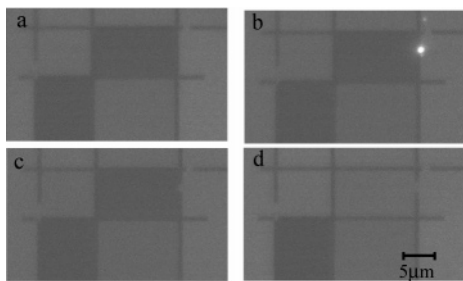


**Figure 2.** (a) An epifluorescence image of a previously optoprotated POPC bilayer (doped with 3 mol % of NBD-PE) showing prominent photobleaching within closed boxes. (b–d) Subsequent healing after perimeter re-illumination using femtosecond pulses at a 540 kHz repetition rate (5 nJ/pulse).

interior of the closed boxes. The open box retains its fluorescence due to lateral exchange of lipid probes with the surrounding bilayer.

Remarkably, when these patterned perimeters are re-illuminated using the same femtosecond laser beam at comparable pulse energies, but at higher repetition rates (200 $\times$ ), we observe local and *instantaneous* removal of these diffusional barriers, suggesting bilayer healing (Figure 2). A previously compartmentalized POPC bilayer is exposed to the Hg illumination until the fluorescence from the corralled bilayer inside the boxes darkened via photobleaching (Figure 2a). Re-illuminating the perimeter of the box using the femtosecond laser beam for  $\sim 1$  s (Figure 2b) at the repetition rate of 540 kHz results in local erasure of the barrier at the site of the illumination (Figure 2c). Within several minutes, the dark interior of the box regains fluorescence (Figure 2d), indicating illumination-induced erasure of diffusional barriers and subsequent exchange of fluorescent lipids with the surroundings. In this manner, barriers to molecular diffusion can be rapidly erected and selectively erased in real time (over large sample areas) without changing the sample or ambient properties.<sup>6</sup> Previously reported healing of bilayers by changing pH should also provide an alternate method for healing optoprotated membranes.

More work is needed to establish the mechanisms which control the writing and erasing of diffusional barriers demonstrated above. Below, we consider key processes at a qualitative, phenomenological level. First, it is now well-established that tightly focused femtosecond pulses can provide sufficiently high local power densities ( $\sim 10^{13}$  W $\cdot$ cm $^{-2}$  at 100 fs) at modest fluences ( $\sim 2$ – $5$  J $\cdot$ cm $^{-2}$ ).<sup>4</sup> This can locally induce plasma formation and material damage even in transparent matter via multiphoton absorption at the laser focus. Above a certain threshold power density, optical breakdown within the material is accompanied by thermal diffusion, shock emission, and cavitation bubble formation causing significant collateral damage in the vicinity of the laser focus.<sup>4,7</sup> In contrast, below this optical breakdown threshold, a low-density plasma is generated within the material which recombines before thermoelastic stresses set in.<sup>4</sup>

In our study, extensive damage observed at pulse energies above 6 nJ is consistent with optical breakdown. Localized modification of lipid bilayers within sub-wavelength dimensions for low pulse energies of 3–6 nJ, however, is suggestive of the formation of a low-density plasma.<sup>4</sup> The latter can directly mediate lipid damage within the laser focus (Supporting Information). Alternatively, plasma formation in water can also cause its dissociation into reactive oxygen species (ROS) such as OH $^{\bullet}$ , H $_2$ O $_2$ , and singlet molecular oxygen.<sup>4</sup> These ROS are highly reactive, have short mean free diffusion path lengths, and cause damage to membrane molecules.<sup>8,9</sup> Interestingly, this process parallels well-known chromophore-assisted laser inactivation (CALI) wherein radical generation occurs due to a comparable multiphoton absorption.<sup>10</sup>

Second, upon local removal of the lipids, the residual membrane does not undergo any major reorganization as judged by the shapes of the voids which reflect the laser beam profile. This observed stability of the void can be attributed to the self-confinement of lipids by local reassembly at the membrane edges forming stable hemi-micellar edge boundaries.<sup>11</sup> Third, the membrane healing, observed upon re-illumination of barrier patterns using femtosecond lasers at high repetition rates, can be understood in terms of thermal effects. At higher repetition rates, the average power deposited within the laser focus is considerable and the dissipation of energy between pulses reduced, resulting in localized heating.<sup>4</sup> This unbinds the bilayer edge and causes expansion at the edges, thereby bridging the width of the diffusional barrier. Such healing should reduce molecular density of the bilayer, placing an upper limit on the number of write/erase cycles. We expect this healing to be dependent on the bilayers' ability to spread upon thermal excitation and thus show a phase state dependence.

In summary, lipid-free gaps, formed by multiphoton absorption due to femtosecond laser illumination, serve as diffusional barriers within the bilayer. Re-illuminating these barriers at comparable peak powers but at higher repetition rates rapidly and selectively erases them via a local, thermal process. Together, this reversible, maskless, multiphoton membrane photolithography provides a new means to compartmentalize and regulate membrane fluidity by erecting and erasing diffusional barriers in real time. We expect that this ability to dynamically alter molecular motions in membranes will better mimic complex dynamics at cellular surfaces and may enable new mechanisms for sorting, separating, and chasing biomolecules.<sup>12</sup>

**Acknowledgment.** We thank N. Banerjee, J. Chan, D. Krol, N. Melikechi, T. Moritz, N. Shen, and M. Yanik for valuable discussions, and NSF Biophotonics Center and DOE (DE-FG02-04ER46173) for financial support.

**Supporting Information Available:** Additional experimental details and supporting figures. This material is available free of charge via the Internet at <http://pubs.acs.org>.

## References

- (1) (a) Vereb, G.; Szollosi, J.; Matko, J.; Nagy, P.; Farkas, T.; Vigh, L.; Matyus, L.; Waldmann, T. A.; Damjanovich, S. *Proc. Natl. Acad. Sci. U.S.A.* **2003**, *100*, 8053–8058. (b) Choquet, D.; Triller, A. *Nat. Rev. Neurosci.* **2003**, *4*, 251–265.
- (2) Jacobson, K.; Sheets, E. D.; Simson, R. *Science* **1995**, *268*, 1441–1442.
- (3) (a) Damjanovich, S.; Gaspar, R.; Pieri, C. *Q. Rev. Biophys.* **1997**, *30*, 67–106. (b) Pralle, A.; Keller, P.; Florin, E. L.; Simons, K.; Horber, J. K. H. *J. Cell Biol.* **2000**, *148*, 997–1007.
- (4) (a) Vogel, A.; Noack, J.; Huttman, G.; Paltauf, G. *Appl. Phys. B* **2005**, *81*, 1015–1047. (b) Vogel, A.; Venugopalan, V. *Chem. Rev.* **2003**, *103*, 577–644.
- (5) (a) Watanabe, W.; Arakawa, N. *Opt. Exp.* **2004**, *12*, 4203–4213. (b) Yanik, M. F.; Cinar, H.; Cinar, H. N.; Chisholm, A. D.; Jin, Y. S.; Ben-Yakar, A. *Nature* **2004**, *432*, 822–822. (c) Tirlapur, U. K.; König, K. *Nature* **2002**, *418*, 290–291. (d) Tirlapur, U. K.; König, K.; Peuckert, C.; Krieg, R.; Halhuber, K. *Exp. Cell Res.* **2001**, *263*, 88–97.
- (6) Previously, lowering of solution pH is used to heal membranes across barriers, albeit it occurs over several hours via changes in substrate hydration properties: (a) Cremer, P. S.; Kung, L. A.; Groves, J. T.; Boxer, S. G. *Langmuir* **1999**, *15*, 3893–3896. (b) Cremer, P. S.; Boxer, S. G. *J. Phys. Chem. B* **1999**, *103*, 2554–2559.
- (7) Schaffer, C. B.; Jamison, A. O.; Mazur, E. *Appl. Phys. Lett.* **2004**, *84*, 1441–1443.
- (8) Wentworth, P.; McDunn, J. E.; Wentworth, A. D.; Takeuchi, C.; Nieva, J.; Jones, T.; Bautista, C.; Ruedi, J. M.; Gutierrez, A.; Janda, K. D.; Babior, B. M.; Eschenmoser, A.; Lerner, R. A. *Science* **2002**, *298*, 2195–2199.
- (9) Yee, C. K.; Amweg, M. L.; Parikh, A. N. *J. Am. Chem. Soc.* **2004**, *126*, 13962–13972.
- (10) Liao, J. C.; Roeder, J.; Jay, D. G. *Proc. Natl. Acad. Sci. U.S.A.* **1994**, *91*, 2659–2663.
- (11) (a) Sens, P.; Safran, S. A. *Europhys. Lett.* **1998**, *43*, 95–100. (b) Jiang, F. Y.; Bourret, Y.; Kindt, J. T. *Biophys. J.* **2004**, *87*, 182–192.
- (12) van Oudenaarden, A.; Boxer, S. G. *Science* **1999**, *285*, 1046–1048.

JA065626P